

Dilution-induced current-density increase in disordered organic semiconductor devices: A kinetic Monte Carlo study

Feiling Yang¹, Harm van Eersel^{2,5}, Jiawei Wang³, Quan Niu^{6,*}, Peter A. Bobbert²,
Reinder Coehoorn^{1,2}, Feilong Liu^{1,†} and Guofu Zhou^{1,4,‡}

¹Guangdong Provincial Key Laboratory of Optical Information Materials and Technology & Institute of Electronic Paper Displays, South China Academy of Advanced Optoelectronics, South China Normal University, Guangzhou 510006, People's Republic of China


²Department of Applied Physics and Institute for Complex Molecular Systems, Eindhoven University of Technology, Eindhoven University of Technology, P.O. Box 513, Eindhoven, Manitoba 5600, Netherlands

³Key Laboratory of Microelectronic Devices and Integrated Technology, Institute of Microelectronics of Chinese Academy of Sciences, Beijing 100029, China

⁴Shenzhen Guohua Optoelectronics Tech. Co. Ltd., Shenzhen 518110, People's Republic of China

⁵Simbeyond B.V., Het Eeuwse 57, Eindhoven, AS 5612, Netherlands

⁶State Key Laboratory of Luminescent Materials and Devices, South China University of Technology, Guangzhou 510640, People's Republic of China

 (Received 9 October 2023; revised 12 December 2023; accepted 20 December 2023; published 25 January 2024)

Using three-dimensional kinetic Monte Carlo simulations, we systematically investigate the effect of dilution with an inert material on the current density in unipolar sandwich-type disordered organic semiconductor devices. Such a dilution technique was studied experimentally by Abbaszadeh *et al.* [Nat. Mater. **15**, 628 (2016)], who observed a dilution-induced increase of the current density. The authors explained the effect as a result of a reduced density of trapped charges (“trap dilution”), assuming an exponential density of trap states. Our simulations support this explanation, and show under which conditions this trap-dilution-induced increase of the current density becomes more than outweighed by the negative effect of the dilution-induced decrease of the mobility. The effect is studied for sets of systematically varied material parameters, including systems with a Gaussian shape of the host and trap DOS.

DOI: [10.1103/PhysRevApplied.21.014050](https://doi.org/10.1103/PhysRevApplied.21.014050)

I. INTRODUCTION

Organic light-emitting diodes (OLEDs) have become one of the key technologies in display applications, such as mobile phones and wearable devices. OLEDs are composed of amorphous disordered molecular semiconductors, resulting from vacuum or solution-based fabrication processes. When a voltage is applied, electrons and holes move through the molecular layers by incoherent hopping in between frontier orbital states that are localized on a molecule. The electrons reside in the lowest unoccupied molecular orbital (LUMO) states and the holes reside in the highest occupied molecular orbital (HOMO) states. Intermolecular interactions give rise to electronic disorder, leading typically to a LUMO and HOMO density of states (DOS) with a Gaussian shape. As a result, low-energy tail states extend into the band gap [1–5].

Experimentally, extrinsic traps are often found to give rise to a superimposed exponential DOS [6–8]. That enhances the density of low-energy tail states, and thereby the trapping of charge carriers, so that the mobility and the current density in devices are reduced. The effect has been investigated in various theoretical [9–12] and experimental [6,7,13] studies. However, in a recent study Abbaszadeh *et al.* found that by diluting a trap-containing organic semiconductor with an inert material, a significant increase of the current density in devices may be obtained [14,15]. For example, in a conjugated polymer blend with 10 wt% of an active semiconductor and 90 wt% of an inert host (with its LUMO and HOMO energies much higher and lower than the active material), the strong electron trapping in the pure conjugated polymer was found to be essentially eliminated [14]. The authors suggested that this “trap dilution” effect can be explained, at least semiquantitatively, by considering that the presence of traps strongly increases the space charge in a device. Under space-charge-limited-current (SCLC) conditions, due to injection from Ohmic or near-Ohmic contacts, a large space charge impedes

*qqniu@scut.edu.cn

†feilongliu@m.scnu.edu.cn

‡guofu.zhou@m.scnu.edu.cn

obtaining a large current density. Trap dilution reduces the trap-induced space charge density and can therefore allow an enhanced current density to be obtained at a given voltage.

As pointed out in Refs. [14,15], a more quantitative analysis of the trap dilution effect may be obtained using the Mark-Helfrich (MH) formula [13], which gives the current density in a unipolar single-layer device with ideal Ohmic contacts, consisting of a disorder-free organic semiconductor that contains traps with an exponentially shaped DOS. We may consider (for definiteness) the electron current density in a unipolar device in which a fraction of f_{dil} inert dilutants has been added to an active semiconductor layer that before dilution consists of a blend of (i) a disorder-free “transport” material with a density $N_{\text{T},0}$ and (ii) charge-trapping molecules with a density $N_{\text{trap},0}$ with an exponential DOS of the form $D(E) = N_{\text{trap},0}/(k_{\text{B}}T_{\text{trap}}) \exp[E/(k_{\text{B}}T_{\text{trap}})]$ for $E < 0$ and $D(E) = 0$ for $E > 0$. The “trap temperature” T_{trap} characterizes the width of the trap DOS, and k_{B} is the Boltzmann constant. At sufficiently large voltages, so that the diffusion contribution to the current density may be neglected, and for temperatures T for which $r \equiv T_{\text{trap}}/T > 1$, an extended version of the MH formula that includes the effect of dilution is then

$$J = Ne\mu(f_{\text{dil}}) \left(\frac{\varepsilon_0\varepsilon_r}{e(1-f_{\text{dil}})N_{\text{trap},0}} \right)^r \frac{V^{r+1}}{L^{2r+1}} C(r), \quad (1)$$

with N the molecular site density, L the layer thickness between the anode and the cathode, $\mu(f_{\text{dil}})$ the dilution-dependent electron mobility in the absence of traps, e the elementary charge, ε_0 the vacuum permittivity, ε_r the relative dielectric permittivity and $C(r) = r'(2r+1)^{r+1}/(r+1)^{2r+1}$. Equation (1) shows that the net effect of dilution on the current density is determined by a balance between the positive effect of trap dilution, because $J \propto 1/[(1-f_{\text{dil}})N_{\text{trap},0}]^r$, and the negative effect due to a decrease of the mobility of the transport material with increasing dilution. As stated in Refs. [14,15], one may therefore expect that a dilution-induced increase of J occurs only when the dimensionless disorder parameter r is sufficiently large. It should also be realized that the basic assumption that underlies Eq. (1), viz., that the transport may be described as trap limited, is expected to become incorrect under strong dilution conditions. A crossover is then expected to a different transport regime, in which all traps are essentially filled.

Trap dilution has been demonstrated experimentally to be a promising method to enhance the current density in organic semiconductor devices, and thus potentially the OLED power efficiency. Analyzing the effect of dilution as observed experimentally can be hampered by various complicating effects, such as the formation of phase-segregated regions and an effect of the dilution on the energetic

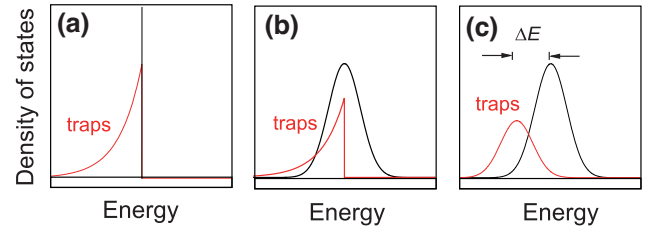


FIG. 1. Electron densities of states (schematic) of the material systems that are studied in this paper. The DOS of the transport material is taken to be a δ function (a) or a Gaussian [(b) and (c)]. The systems have a superimposed exponential electron trap DOS [(a) and (b)], or a Gaussian trap DOS (c). The trap DOS can be taken to be shifted by an energy ΔE with respect to that of the transport material. The electron DOS of an inert diluting material does not overlap with these distributions, and is not shown.

disorder of the frontier orbital states of the constituent molecules [14].

It is therefore of interest to study the effect using a modeling method that more realistically describes the charge transport than assumed in the analysis that has led to Eq. (1) and that avoids possible uncertainties concerning the molecular-scale structure and energetic disorder that can complicate the analysis of experimental results.

In this paper, we present a comprehensive investigation of the effect of dilution on the current density in devices of disordered organic semiconductors. Using a three-dimensional (3D) kinetic Monte Carlo (KMC) approach, we model the dilution effect by assuming random and spatially uncorrelated 3D molecular-scale mixing of the active transport material, the trap molecules, and the inert host molecules. Figure 1 gives an overview of the types of systems studied: (a) a disorder-free (δ -function-shaped) DOS and an exponential trap DOS, (b) a Gaussian DOS with an exponential trap DOS, and (c) a Gaussian DOS with a Gaussian trap DOS. Situation (a) represents the shape of the DOS that has been assumed when deriving Eq. (1), with a disorder-free transport material. In situation (b), the shape of the DOS of the transport material is more realistic. Situation (c) represents the shape of the DOS that is usually assumed when considering host-guest systems, in which a small concentration of guest molecules that act as traps is added to the transport (host) material.

We furthermore study the sensitivity to the degree of dilution, the layer thickness and the measurement conditions (voltage and temperature) and to the average hop distance (by varying the electron wave-function decay length). The analysis goes therefore well beyond the one-dimensional drift-only approach assuming a zero-disorder host material that has been used to derive Eq. (1). In particular, the use of 3D KMC simulations allows the percolative nature of the charge-transport process to be properly captured, which, especially in the case of diluted systems, is

sensitive to the interaction range between the randomly dispersed active material molecules.

The paper is structured as follows. Section II gives a description of the KMC simulation model used in this work. Section III discusses the crossover from the trap limited to the trap-filled transport regime that is expected upon dilution. The analysis is used in Sec. IV, in which the simulation results are presented and discussed for the case of transport material without energetic disorder and with an exponential trap DOS. Simulation results for a transport material with a Gaussian DOS and an exponential or Gaussian trap DOS are given in Sec. V. Section VI summarizes the conclusions and gives an outlook to the next steps.

II. MATERIAL AND SIMULATION MODEL

The simulations are carried out using the 3D KMC simulation tool Bumblebee [16]. As the simulation methodology is analogous to that in earlier 3D KMC studies of the transport in disordered semiconductor materials and devices (see, e.g., Refs. [17–20]), we focus here on the specifics of the three-component systems that are studied in this work. We consider sandwich-type 100-nm-thick devices within which the molecules are located on simple cubic lattice sites with an intersite distance $a = N^{-1/3}$, with $a = 1$ nm. The molecular sites are randomly taken to be either a transport site, a trap site, or a diluting molecule site, with volumetric densities N_T , N_{trap} , and N_{dil} , respectively, such that $N_T + N_{\text{trap}} + N_{\text{dil}} = N$. The volumetric densities of the charge carriers that occupy these sites are denoted as n_T , n_{trap} , and n_{dil} , respectively. The transport and trap sites are called “active.” Upon dilution, the fraction of active sites is decreased while keeping the ratio of transport and trap sites fixed. We define the charge-carrier concentrations per active molecular site as $c_{\text{act}} = (n_T + n_{\text{trap}})/(N_T + N_{\text{trap}})$ and per total molecule site as $c_{\text{tot}} = (n_T + n_{\text{trap}})/(N_T + N_{\text{trap}} + N_{\text{dil}})$, respectively.

We consider only electron transport. For trap sites with an exponential trap DOS, the LUMO levels are taken from a normalized distribution

$$D_E(E) = \begin{cases} \frac{1}{k_B T_{\text{trap}}} \exp\left(\frac{E - E_{0,E}}{k_B T_{\text{trap}}}\right), & \text{for } E \leq E_{0,E}, \\ 0, & \text{for } E > E_{0,E}, \end{cases} \quad (2)$$

where $E_{0,E}$ is the upper boundary of the distribution and $k_B T_{\text{trap}}$ is the distribution width. For trap sites with a Gaussian DOS, the LUMO levels are randomly taken from a normalized distribution

$$D_G(E) = \frac{1}{\sqrt{2\pi}\sigma} \exp\left(-\frac{(E - E_{0,G})^2}{2\sigma^2}\right), \quad (3)$$

with $E_{0,G}$ and σ the mean value and standard deviation (width) of the distribution, respectively.

The electrons are assumed to be localized on individual molecular sites and move between different sites via

hopping processes. The electron hopping rate ω_{ij} from molecule i to molecule j is assumed to be described by the Miller-Abrahams formula [21]

$$\omega_{ij} = \nu_1 \exp\left[-\frac{2(R_{ij} - a)}{\lambda}\right] \exp\left(-\frac{|\Delta E_{ij}| + \Delta E_{ij}}{2k_B T}\right), \quad (4)$$

with R_{ij} the distance between the molecular sites i and j , ν_1 the nearest-neighbor (NN) hopping attempt rate, λ the wave-function decay length, and $\Delta E_{ij} = E_j - E_i$ the energy difference between sites i and j . The site energies E_i are determined by the DOS, the external electric field, the Coulomb interactions with the other electrons and the image charges in the electrodes.

The diluting material is assumed to have a LUMO energy that is much higher than that of the active material and the trap molecules, so that no electron transfer is possible to these molecules. The value of λ will be varied, with a default value of 0.5 nm. To ensure that long-distance hopping is accurately included, hops over distances R_{ij} up to $5a$ are included. We note that the KMC simulation model does not exclude direct transfer of electrons between trap states. However, at small trap densities such direct transfer processes are rare.

The size of a typical 3D KMC full-device (FD) simulation box is $100 \times 100 \times 100$ nm³, with electrode interfaces at $x = 0$ nm and $x = L$. Periodic boundary conditions are assumed in the y and z directions. The electrodes are treated as ideal conductors, with a Fermi energy that is 0.2 eV below the average LUMO energy of the active organic semiconductor material. In such a case, the injection process is known to be ideally Ohmic [22]. The charge injection and collection rates are described by a Miller-Abrahams-type expression that is analogous to Eq. (4).

In addition to device simulations, also simulations with fully periodic boundary conditions (PBCs) were carried out for mobility calculations. The default box size was also $100 \times 100 \times 100$ nm³. However, when needed for obtaining a sufficient statistical accuracy larger systems were taken. The drift-only current density that follows from such simulations, which are performed for a fixed electron carrier density n and for a uniform electric field F_x in the x direction, provides the electron density and field dependence of the mobility function, $\mu(n, F)$.

Both FD and PBC simulations are terminated when the system reaches steady state, i.e., the current fluctuation due to KMC events becomes smaller than 4%. To minimize the inaccuracy of the simulation results due to randomness in energy landscape, the results that are shown in this paper are an average of typically five disorder configurations.

An overview of the default material and device parameters is given in Table I. The default value of the fraction of traps ($f_{\text{trap}} \equiv N_{\text{trap}}/(N_T + N_{\text{trap}})$) is 0.01, which is at the upper boundary of the range of experimental values for

TABLE I. Overview of the default material and device parameters of the device type that is shown in Fig. 1(a). The parameters that are given in the first (“common”) part of the table are also used when studying the device types that are shown in Figs. 1(b) and 1(c).

Parameter	Value
Common parameters	
Intermolecular distance a	1 nm
NN hopping attempt rate ν_1	$3.3 \times 10^{10} \text{ s}^{-1}$
Relative dielectric permittivity ϵ_r	3
Wave-function decay length λ	0.5 nm
Layer thickness L	100 nm
Temperature T	290 K
Voltage V	5 V
DOS transport material	
DOS width σ	0 eV
Peak offset energy ΔE	0 eV
Exponential trap DOS	
Characteristic trap temperature T_{trap}	1500 K
Fraction of traps,	
$f_{\text{trap}} \equiv N_{\text{trap}}/(N_T + N_{\text{trap}})$	0.01
Upper boundary distribution $E_{0,E}$	0 eV

small-molecule organic semiconductors and conjugated polymers. The assumed characteristic trap temperature T_{trap} is 1500 K, whereas typical values vary from 1000 to 2500 K [6,14,17,23].

III. TRANSPORT REGIMES

Before presenting the simulation results in the next section, it is useful to analyze under which conditions the transport in SCLC devices is determined by the presence of trap states, and how the role of trapping is changed by dilution. A simple criterion may be obtained using a result by Lampert and Mark [24], who proved that for unipolar devices that operate under SCLC conditions at a sufficiently large voltage, so that the contribution of diffusion to the charge and current density may be neglected, the layer-averaged charge carrier density is given by

$$n_{\text{av}} = \alpha \frac{\epsilon_0 \epsilon_r V}{eL^2}. \quad (5)$$

Here, α is a numerical factor in the range 1–2 that depends on the details of the system. Equation (5) expresses that under the conditions mentioned above the average bulk charge density is (within a factor of 2) obtained by distributing the areal charge density on the plates of a capacitor with equal thickness ($\epsilon_0 \epsilon_r V/L$) over the full device thickness.

When studying devices that are based on a diluted organic semiconductor with trap states, one may expect that most of the injected carriers are trapped when

$$n_{\text{av}} < N_{\text{trap}} \equiv (1 - f_{\text{dil}})N_{\text{trap},0}, \quad (6)$$

i.e., when

$$\alpha \frac{\epsilon_0 \epsilon_r V}{eL^2} < (1 - f_{\text{dil}})N_{\text{trap},0}. \quad (7)$$

When all traps are filled, the effect of further dilution is a decrease of the current density, resulting from the dilution-induced decrease of the mobility. From Eq. (7), the critical fraction of dilutants, above which the system is in the trap-filled transport regime, is given by

$$f_{\text{dil,crit}} \approx 1 - \alpha \frac{\epsilon_0 \epsilon_r V}{eL^2 N_{\text{trap},0}}. \quad (8)$$

For the default device parameters, given in Table I, $f_{\text{dil,crit}} = 0.983 - 0.992$ (depending on α). Trap filling is then thus expected to occur only for very large dilution levels, and simulation results for smaller value of f_{dil} are expected to probe how well Eq. (1) provides an appropriate expression for the current density in the trap-limited current regime. However, for a trap concentration that is a factor of 10 smaller than the default value, the trap filling is expected to occur already at much smaller dilution fractions, viz., in the range of 0.83–0.92. We study the effect of dilution for various trap densities in the next section.

We note that the analysis that has been given in this section neglects the actual nonuniformity of the charge-carrier density profile across the layer thickness, which even occurs in the absence of a diffusion contribution to the current density. In addition, charge-carrier diffusion enhances the carrier density near the electrodes. Close to the electrodes, the trap-filled limit is therefore already reached at smaller dilution fractions than as given by Eq. (8).

IV. RESULTS AND DISCUSSION—NONDISORDERED TRANSPORT MATERIAL

In this section, we consider devices that are based on a material with a DOS, such as shown in Fig. 1(a), with the set of default parameters that is given in Table I. The effect of dilution on the current density is presented in subsection A, and is analyzed in subsection C using an approximate model that employs expressions for the composition, electron density and field dependence of the mobility that are developed in subsection B. In subsection D, the resulting approximate model is used to analyze the calculated sensitivity of the $J(f_{\text{dil}})$ curves to parameter variations.

A. Device simulations—current density enhancement for the default device

Figure 2(a) shows how for the default device the current density at $V = 5 \text{ V}$ is enhanced when diluting the system. For the undiluted system, the current density is

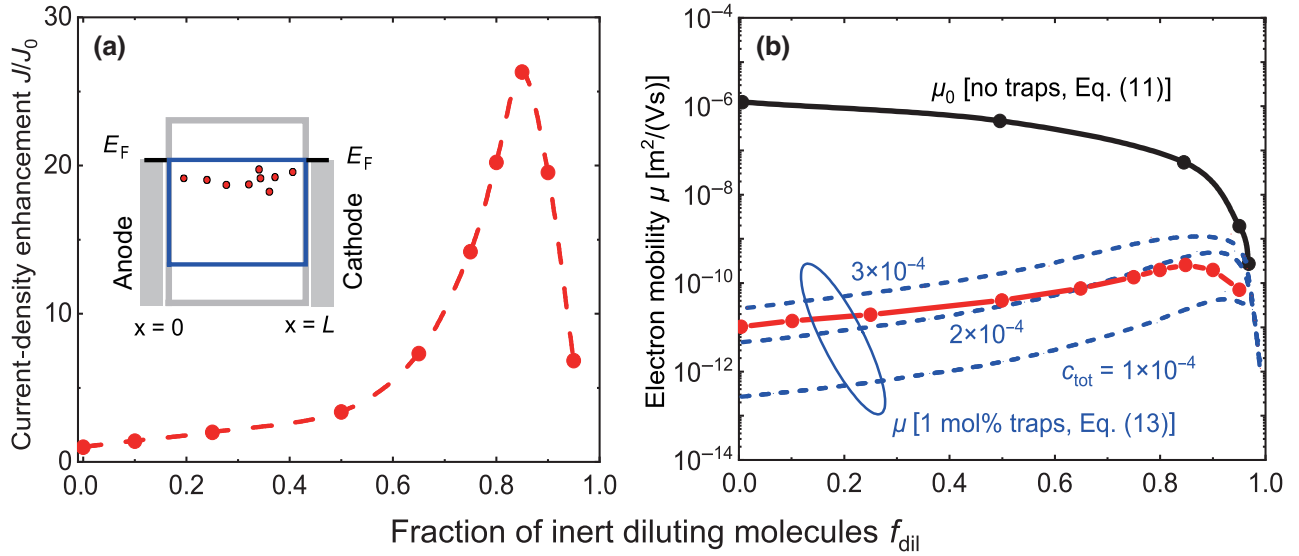


FIG. 2. (a) Effect of dilution by inert host molecules on the current density J , normalized by its predilution value J_0 , for a device with a DOS as shown in Fig. 1(a) and with parameters as given in Table I, calculated using 3D KMC FD simulations. The inset shows the schematic flat-band energy-level diagram. The material blend that is sandwiched in between the two electrodes is composed of a transport material with a δ -function-shaped DOS (blue colored box), trap molecules with an exponentially shaped DOS traps (red colored spheres), and an inert host (gray colored box). (b) Effect of dilution on the mobility at a field $F = 5 \times 10^7$ V/m in a trap-free material (black full curve and symbols) and in a material containing traps, as specified in Table I (blue dashed curves). The curves are obtained using Eqs. (11) and (13), as indicated in the figure and as discussed in the text. The red full curve and symbols show a mobility curve with an f_{dil} dependence that is equal to the ratio J/J_0 that is shown in panel (a). The mobility increase with f_{dil} that is shown by the blue dashed curves is somewhat different from the increase of the current density that is shown by the red curve and symbols due to (i) a variation of c_{tot} and F throughout the device, and (ii) a variation with f_{dil} of the contribution of direct-trap-to-trap transport.

$J = 120$ A/m². It increases with dilution until a maximum of $J \cong 3200$ A/m² is reached for a dilutant fraction of $f_{\text{dil}} \sim 0.84$. Further dilution leads to a decrease of the current density. This simulation result is qualitatively in agreement with experimental observations [14].

The finding of an initial enhancement of the current density upon dilution, followed by a decrease, can be understood by considering the effect of dilution on the (position-dependent) charge-carrier density, mobility, and electric field. Figures 3(a) and 3(b) show the charge-carrier density profiles for the transport and trap sites (n_{T} and n_{trap}) at various dilution fractions f_{dil} . The density of carriers on transport sites shows an increase upon dilution, while the trapped carrier density shows a (much weaker) opposite trend. Whereas in undiluted systems n_{T} is approximately 4 orders of magnitude smaller than n_{trap} , dilution to a fraction of host molecules of 95% leads to approximately equal electron densities.

The device performance may be analyzed by focusing on the trapped and free carrier densities and the electric field in the device center ($x = L/2$), which are given in Table II. The table shows that the total carrier concentration in the device center, $c_{\text{tot,ctr}}$, changes only weakly upon dilution and falls in the range $(1.4\text{--}2.1) \times 10^{-4}$. This concentration range overlaps with the range $(0.8\text{--}1.6) \times 10^{-4}$

that would be expected from Eq. (5), with $\alpha = 1 - 2$. Equation (5) neglects the role of diffusion, which will lead to an enhanced average carrier density, and gives the device-averaged concentration instead of the value at the device center. In view of that, the agreement may be regarded as fair. For effective values of α in the range 2–3, one expects from Eq. (5) that all traps are essentially filled for $f_{\text{dil,crit}} \approx 0.98$. The simulation results in Table II show that in the entire f_{dil} range studied, up to a value of 0.95, the traps are far from being filled completely. The finding of a distinct decrease of the current density at high dilution fractions and a peak in the current density that already occurs at $f_{\text{dil}} \approx 0.85$ implies that the electron mobility in the trap-free transport material actually decreases strongly with increasing dilution. This will be studied in the next subsection.

B. Mobility—simulations and models

Figure 4(a) shows for four dilution levels the calculated mobility for the organic semiconductor with the default composition of transport and trap sites, as a function of the active-site-normalized electron concentration c_{act} . The simulations have been carried out for the average electric field across the devices that are studied ($F = V/L = 5 \times 10^7$ V/m). By presenting the mobility as a function

TABLE II. Analysis of the current-density enhancement for the default device [see Table I and Fig. 2(a)] for selected values of the dilutant fraction f_{dil} , using the KMC simulation results in the device center. The electron densities in transport and trap sites in the device center, $n_{\text{T,ctr}}$ and $n_{\text{trap,ctr}}$, respectively, have been taken from Figs. 3(a) and 3(b), respectively. The last column gives the current density that has been obtained from the 3D KMC FD simulations.

f_{dil}	$n_{\text{T,ctr}}$ (m^{-3})	$n_{\text{trap,ctr}}$ (m^{-3})	$n_{\text{T,ctr}} + n_{\text{trap,ctr}}$ (m^{-3})	$\frac{n_{\text{trap,ctr}}}{N_{\text{trap}}}$	$c_{\text{act,ctr}}$ (10^{-4})	$c_{\text{tot,ctr}}$ (10^{-4})	F_{ctr} (10^7 V/m)	μ_{ctr} [$\text{m}^2/(\text{Vs})$]	$J_{\text{device,ctr}}$ (A/m^2) Eq. (15)	$J_{\text{device,KMC}}$ (A/m^2)
0	1.8×10^{19}	2.0×10^{23}	2.0×10^{23}	0.020	2.0	2.0	5.6	$(4 - 9) \times 10^{-11}$	70 – 160	120
0.5	1.2×10^{20}	1.8×10^{23}	1.8×10^{23}	0.036	3.6	1.8	5.5	$(2 - 4) \times 10^{-10}$	310 – 630	400
0.85	7×10^{21}	1.4×10^{23}	1.4×10^{23}	0.093	9.3	1.4	5.4	$(1 - 3) \times 10^{-9}$	1200 – 3600	3160
0.95	6×10^{22}	8×10^{22}	1.4×10^{23}	0.16	28	1.4	5.1	$(3 - 9) \times 10^{-10}$	340 – 1030	820

of c_{act} , we focus on the negative effect on the mobility that would occur by an (effectively diluting) expansion of the system, without adding or removing charges from the active sites. The mobility functions show a strong increase with c_{act} , which will be analyzed below in detail, until the trap-filled limit is reached around $c_{\text{act}} \approx f_{\text{trap}} = 10^{-2}$.

In Fig. 4(b), the same simulation data are presented as a function of the total electron concentration, c_{tot} . This

view on the effect of dilution is motivated by the finding, in the previous subsection, that upon dilution the total electron concentration is almost independent of the dilution fraction. The gray zone in the figure gives the range of typical concentrations in the device center (see Table II). For such a fixed value of c_{tot} , the mobility is seen to increase with increasing dilution, until for $f_{\text{dil}} \approx 0.85$ a decrease sets in due to the combined effects of trap filling and a further decrease of the mobility in the diluted trap-free material. This picture provides thus a clear, at least qualitative, explanation for the finding of a maximum of the current density enhancement around $f_{\text{dil}} = 0.85$ (see Fig. 2). A more quantitative model will be developed in the next subsection, using a more in-depth analysis of the electron concentration and f_{dil} dependence of the mobility.

At small electron concentrations, the mobility is to an excellent approximation linear on the double-log scale used. Such a result is expected for a wide trap distribution ($T \ll T_{\text{trap}}$, with E_{F} the Fermi energy, expressed with respect to the energy of the transport states), and for small trap densities ($N_{\text{trap}} \ll N$), when the system is close to thermal equilibrium, i.e., for sufficiently small fields. The electron densities on the trap and transport materials are then given by $n_{\text{trap}} \cong N_{\text{trap}} \exp(E_{\text{F}}/(k_{\text{B}}T_{\text{trap}}))$ [25] and $n_{\text{T}} \cong N_{\text{T}} \exp(E_{\text{F}}/(k_{\text{B}}T))$, respectively. Their relationship may be expressed as $n_{\text{T}} \cong N_{\text{T}}(n_{\text{trap}}/N_{\text{trap}})^{T_{\text{trap}}/T} = N_{\text{T}}(n_{\text{trap}}/N_{\text{trap}})^r$ and their ratio is given by

$$\frac{n_{\text{T}}}{n_{\text{trap}}} = \frac{N_{\text{T}}}{n_{\text{trap}}} \left(\frac{n_{\text{trap}}}{N_{\text{trap}}} \right)^r = \left(\frac{N_{\text{T}}}{N_{\text{trap}}} \right)^r \left(\frac{n_{\text{trap}}}{N_{\text{T}}} \right)^{r-1} \cong \frac{c_{\text{act}}^{r-1}}{f_{\text{trap}}^r}, \quad (9)$$

assuming that $f_{\text{trap}} \ll 1$. The mobility is expected to be given by the concentration of charge carriers in transport states, multiplied by the mobility $\mu_0(f_{\text{dil}})$ of charge carriers in the diluted but trap-free transport material. For small electron concentrations, when most charges occupy trap states, the mobility is from Eq. (9) then to a good

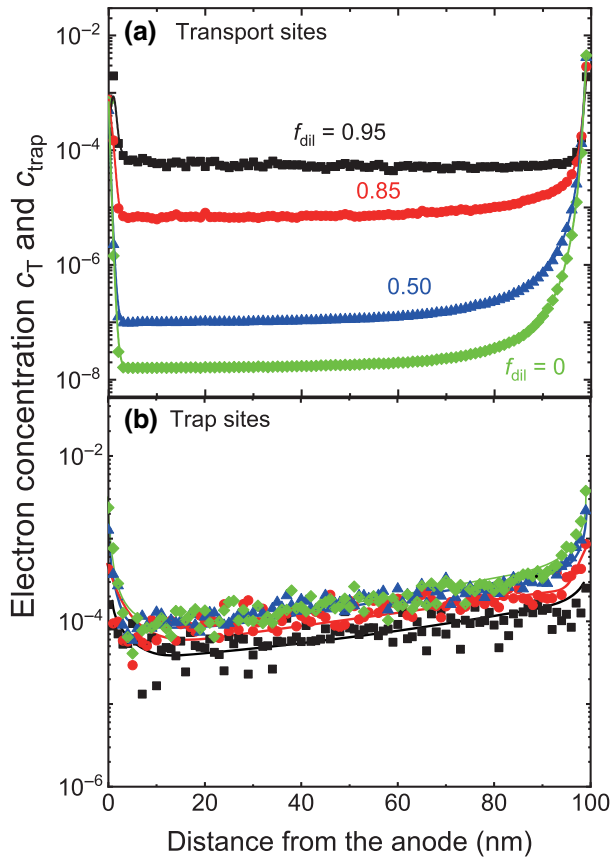


FIG. 3. Profiles of the electron concentration calculated using 3D KMC FD simulations on (a) transport sites (c_{T}) and (b) trap sites (c_{trap}), for the device shown in Fig. 1(a), at various dilution fractions f_{dil} . The legends to the curves that are given in (a) apply also to (b).

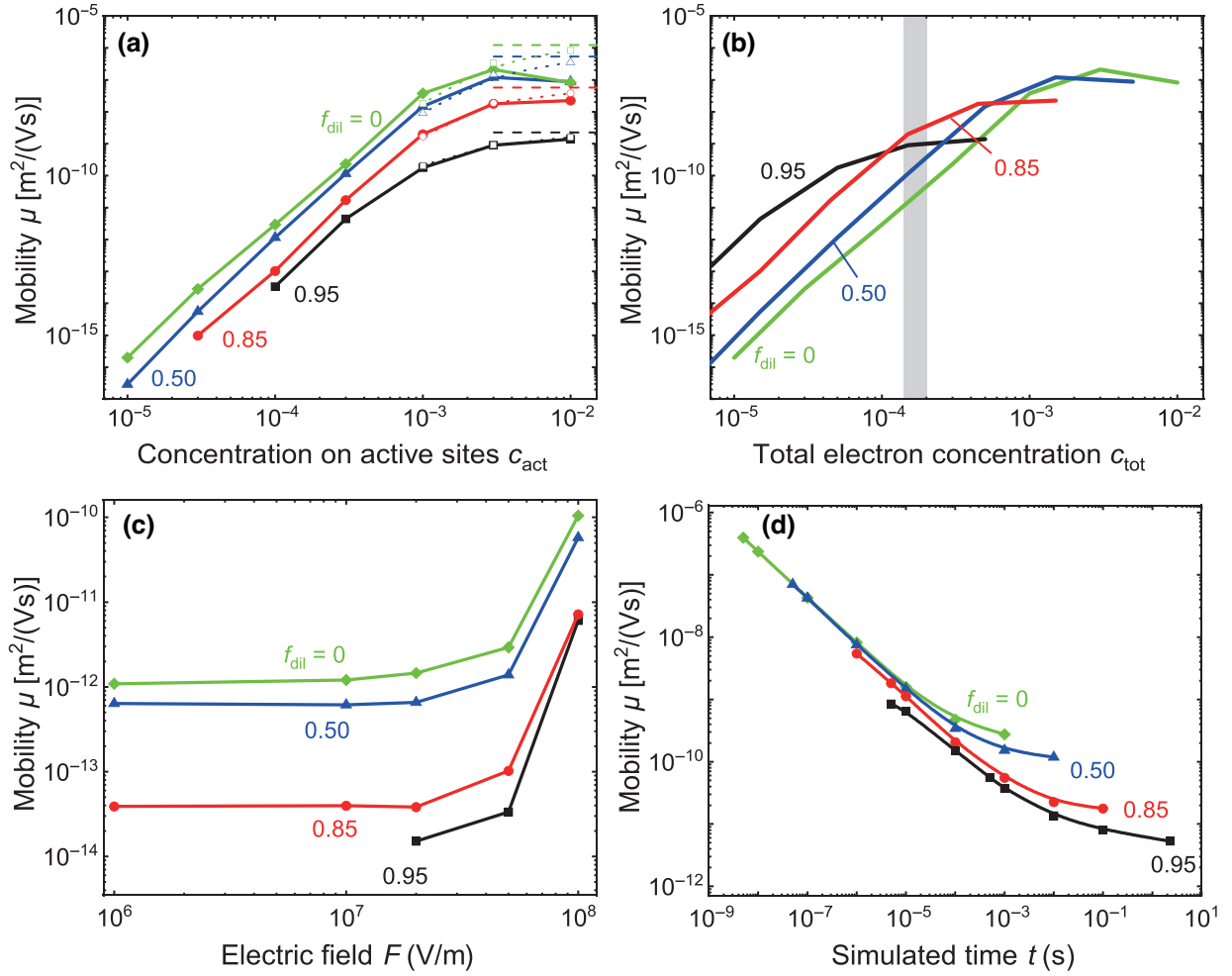


FIG. 4. Charge-carrier mobility, obtained from 3D KMC PBC simulations, for systems with an exponential trap DOS as specified in Table I (full curves and filled symbols). (a),(b) Dependence of the steady-state mobility on the concentration on active sites, c_{act} [panel (a)], and the total electron concentration, c_{tot} [panel (b)], at an electric field $F = 5 \times 10^7$ V/m. (c) Electric field dependence of steady-state mobility at $c_{act} = 10^{-4}$. (d) Simulated time evolution of the mobility in the KMC simulations, resulting from carrier relaxation, at $F = 5 \times 10^7$ V/m and $c_{act} = 3 \times 10^{-4}$. In panel (a), the dotted curves and open symbols are mobilities neglecting Coulomb correlation. The dashed lines show the trap-free limit of mobilities. In panel (b), the gray zone indicates the range of typical values of c_{tot} in the center of the default devices containing these materials (see Table II).

approximation given by

$$\begin{aligned} \mu(c_{act}, f_{trap}, f_{dil}, F) &= \frac{n_T}{n_T + n_{trap}} \mu_0(f_{dil}, F) \\ &\cong \frac{c_{act}^{r-1}}{f_{trap}^r} \mu_0(f_{dil}, F). \end{aligned} \quad (10)$$

The slope of the mobility curves in Fig. 4(a) is for small c_{act} thus expected to be $(r-1) \approx 4.17$, which agrees excellently with the simulation results.

The dilution effect is due to an increase of the average distance between the transport sites and due to their positional disorder. In the absence of traps, and neglecting positional disorder, an increase of the intermolecular distance to an effective value $a(f_{dil}) = a/(1-f_{dil})^{1/3}$ would

[using Eq. (4)] lead an f_{dil} dependence of the mobility of the form

$$\begin{aligned} \mu_0(f_{dil}, F) &= \sum_{i,j,k} \exp \left[\frac{-2 \left(\frac{(i^2+j^2+k^2)^{1/2}}{(1-f_{dil})^{1/3}} - 1 \right) a}{\lambda} \right] \\ &\exp \left[\frac{eFa(i-|i|)}{(1-f_{dil})^{1/3} 2k_B T} \right] \frac{iav_1}{(1-f_{dil})^{1/3} F}, \end{aligned} \quad (11)$$

where the summation includes contributions due to hopping from a site $(0,0,0)$ (which is excluded from the summation) to molecules with integer site indices i, j , and k . This approximation has been used in earlier work [see Eq. (1) of Ref. [26] and references therein], where the site

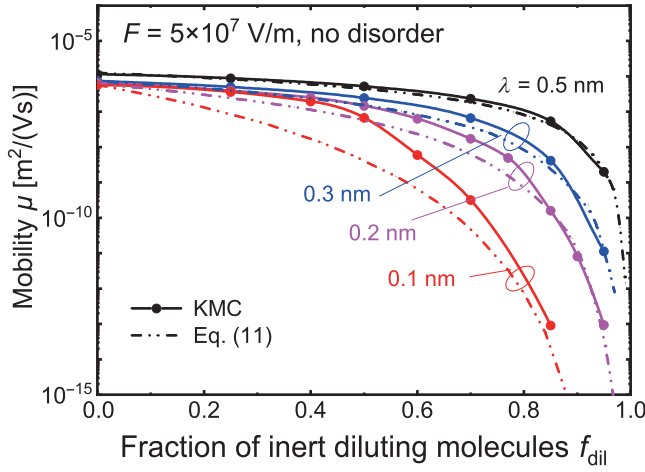


FIG. 5. Charge-carrier mobility for systems that consist of a transport material with a δ -function-shaped DOS that is diluted by a mol fraction f_{dil} of an inert material, for various values of the wave-function decay length λ , studied at a field of $F = 5 \times 10^7$ V/m. Dashed curves show the f_{dil} dependence that is predicted by Eq. (11) and symbols and full curves show the results of 3D KMC PBC simulations. The results for $\lambda = 0.5$ nm are used in Secs. IV C and IV D.

density dependence of the mobility was described by

$$\mu \propto \exp \left[-\frac{C}{(1-f_{\text{dil}})^{1/3}} \frac{a}{\lambda} \right], \quad (12)$$

with $C \approx 2$. We find that for the default values of a , T , and F (see Table I), Eq. (12) provides an excellent description for the shape of the function μ_0 that is described in Eq. (11) when taking $C = 1.9$. Figure 5 shows that KMC simulation results for $\mu_0(f_{\text{dil}}, F)$, with $F = 5 \times 10^7$ V/m, a small carrier concentration ($c = 10^{-4}$) and $\lambda = 0.5$ nm (black curve) are for the entire range of f_{dil} values well described by Eq. (11). The effect of positional disorder is then thus negligible. For smaller values of λ , differences between the mobilities as obtained from the model (dashed curves) and the KMC simulation results (symbols and full curves) are visible, in particular for $\lambda = 0.1$ nm. The mobility can then be enhanced as compared to the values that are predicted by Eq. (11) due to percolative transport via rare paths that are formed by molecules with smaller-than-average intermolecular distances.

For electron concentrations for which most trap states are filled, the mobility is given by the following more general expression:

$$\begin{aligned} \mu(c_{\text{act}}, f_{\text{trap}}, f_{\text{dil}}, F) &= \frac{n_{\text{T}}}{n_{\text{T}} + n_{\text{trap}}} \mu_0(f_{\text{dil}}, F) \\ &= \frac{1}{1 + \frac{N_{\text{trap}} \exp(E_{\text{F}}/(k_{\text{B}}T_{\text{trap}}))}{N_{\text{T}} \exp(E_{\text{F}}/(k_{\text{B}}T))}} \mu_0(f_{\text{dil}}, F), \end{aligned} \quad (13)$$

where E_{F} is a function of c_{act} that may be obtained from the implicit expression

$$c_{\text{act}} = \frac{N_{\text{T}} \exp\left(\frac{E_{\text{F}}}{k_{\text{B}}T}\right) + N_{\text{trap}} \exp\left(\frac{E_{\text{F}}}{k_{\text{B}}T_{\text{trap}}}\right)}{N_{\text{T}} + N_{\text{trap}}}. \quad (14)$$

The dependence of the mobility on the total electron concentration, c_{tot} , follows straightforwardly by using the relationship $c_{\text{tot}} = (1 - f_{\text{dil}})c_{\text{act}}$. In the low and high concentration limits, the function that is given by Eq. (13) extrapolates to the low-concentration and high-concentration expressions that are given by Eqs. (10) and (11), respectively.

The calculated mobility in trap-free materials is in Fig. 4(a) indicated by dashed horizontal lines near the right-hand axis of the figure. For the two strongly diluted systems ($f_{\text{dil}} = 0.85$ and 0.95), the mobility curves indeed approach $\mu_0(f_{\text{dil}}, F)$ asymptotically when x_{act} approaches the fraction of traps (0.01). However, for the two other systems that are considered ($f_{\text{dil}} = 0$ and 0.5), the mobility curves show a maximum around $c_{\text{act}} \approx 3 \times 10^{-3}$. We attribute the subsequent decrease to Coulomb correlation effects, similar to those found from KMC simulations for transport in a Gaussian DOS [27,28]. That is supported by simulation results that are obtained after switching off the electron-electron Coulomb interaction (open symbols and dotted curves). For the two strong dilution cases studied ($f_{\text{dil}} = 0.85$ and 0.95), a value of c_{act} close to 0.01 corresponds to a much smaller fractional occupation of all sites, so that Coulomb correlation effects are only weak.

The field dependence of the mobility in a system containing traps would, from Eq. (10), be expected to be negative, because of the negative field dependence of the mobility in the transport material [Eq. (11)]. However, the field dependence of the mobility in systems containing traps is actually positive, as shown in Fig. 4(c). The effect is due to direct trap-to-trap transport, which is possible due to the use of a relatively large wave-function decay length (0.5 nm). We also remark that in the presence of traps, the development of a proper dynamic thermal equilibrium can take a long time. Figure 4(d) shows, as an example, the time dependence of the mobility that is obtained from KMC simulations for a concentration $c_{\text{act}} = 3 \times 10^{-4}$ after populating at time $t = 0$ randomly selected active material sites. The relaxation process is seen to be particularly slow for strongly diluted systems. This implies that one should be careful when using mobility functions such as shown in Fig. 4(a) when analyzing the charge transport in devices under conditions that do not allow full relaxation (e.g. low device thickness, high energetic disorder, and large trap fractions).

We can now evaluate the accuracy with which Eq. (10) predicts the sensitivity of the mobility to the presence

of traps. As an example, we consider a nondiluted system, studied at $F = 5 \times 10^7$ V/m [diamond symbols and green curve in Fig. 4(a)]. Using the value of $\mu_0(0, F) = 1.3 \times 10^{-6}$ m²/(Vs) that follows from Eq. (11), one would expect from Eq. (10) that the addition of 1 mol% of traps decreases the mobility for $c_{\text{act}} = 10^{-4}$ to 6×10^{-13} m²/(Vs). However, the simulated value is a factor of approximately 6 larger, viz., $(3 \pm 1) \times 10^{-12}$ m²/(Vs). We attribute the difference partly to the occurrence of direct trap-to-trap hopping, which is [from Fig. 4(c)] further enhanced by the application of the electric field. A 3D KMC PBC simulation with trap-to-trap hopping turned off reduces in this case the mobility to $(1.5 \pm 0.4) \times 10^{-12}$ m²/(Vs). The other source of the difference is the Coulomb correlation between the charge carriers, as shown in Fig. 4(a). A 3D KMC PBC simulation with both Coulomb correlation and trap-to-trap hopping turned off in this case then further reduces the mobility to $(7 \pm 2) \times 10^{-13}$ m²/(Vs), in agreement with the theoretical prediction. We will include these effects in a phenomenological manner in the model for the current density in devices that is developed in the next subsection.

C. Approximate model of the current-density enhancement

It is of interest to investigate to what extent the sensitivity of the current-density enhancement to variations of the material parameters and measurement conditions could be predicted without performing KMC simulations. We first note that an analysis in Table II shows that the dilution-dependent current density in the default devices is fairly well described within a simple drift-only model,

$$J = J_{\text{device,ctr}} \approx n_{\text{tot,ctr}} e \mu_{\text{ctr}} F_{\text{ctr}}, \quad (15)$$

that utilizes the calculated electron density ($n_{\text{tot,ctr}}$) and field (F_{ctr}) in the device center and the corresponding mobility (μ_{ctr}) that is obtained from the density and field dependence of the mobility function in Figs. 4(a) and 4(b). We note that the accuracy of this analysis is hampered by the stochasticity of the free and trapped electron densities (see Fig. 3). That translates into relatively large uncertainty intervals of the corresponding mobility and current density.

We can then make use of the finding (see Sec. IV A and Table II) that the electron density in the device center is only weakly dependent of f_{dil} and close to the value that is expected from Eq. (5), and that the field in the device center is fairly well approximated by the device-averaged field, V/L . Within the approximations made, the dilution-dependence of the current density is then only dependent on the dilution-dependence of mobility in the device center.

In Fig. 2(b), this approximation is applied to the default devices. The full black curve, obtained using Eq. (11), shows how in the absence of traps the mobility in the

device center would decrease monotonically with increasing dilution. However, in the presence of 1 mol% of traps an initial mobility increase is expected, followed by a decrease at high dilution levels [dashed blue curves, from Eq. (13)]. Curves for three values of the total electron concentration in the device center are given, in the range $c_{\text{tot,ctr}} = (1-3) \times 10^{-4}$ that corresponds to $\alpha = 1.2-3.6$. This overlaps with the range of simulated electron concentrations in the device center $((1.4-2.0) \times 10^{-4})$. A larger value of $c_{\text{tot,ctr}}$ is expected to lead to a smaller value of the critical dilution fraction at which a transition to the trap-filled regime takes place [see Eq. (8)]. The three curves indeed show that with increasing $c_{\text{tot,ctr}}$ the peak in the current density shifts to smaller values of the dilution fraction.

The red full curve in Fig. 2(b) shows the relative increase $J(f_{\text{dil}})/J(f_{\text{dil}} = 0)$ of the current density, taken from Fig. 2(a) and normalized by an arbitrarily chosen factor of 1×10^{-11} m²/(Vs). The comparison shows that the model predicts a somewhat steeper increase of the current density and a somewhat larger value of the dilution fraction, $f_{\text{dil,max}}$, for which the current density is largest. The differences may be attributed to the various approximations that have been made, including the variation of the total charge density and the field with f_{dil} and including a variation of the contribution of direct-trap-to-trap transport with f_{dil} , as discussed in Sec. IV A. The latter effect leads to an enhanced mobility for small f_{dil} , but becomes relatively small when for large f_{dil} most transport is due to hops of electrons between transport states. The value of $f_{\text{dil,max}}$ is therefore expected to be smaller than as predicted by Eq. (13), consistent with the observed discrepancy.

An overall conclusion from this analysis is that the maximum possible enhancement of the current density that can be realized by dilution depends on a subtle balance between various effects. (i) The current density increases initially due to an increase of the density of highly mobile electrons on transport sites. However, this increase ends when the trap-filled limit has been reached. And before that limit has been reached, (ii) the dilution-induced decrease of the mobility of electrons on transport sites can already limit the maximum possible current density increase.

D. Sensitivity studies

We have studied the sensitivity of the current-density enhancement to a variation of five parameters. Figures 6(a)–6(e) shows the KMC simulation results (symbols and full curves), and the results that are expected from the model that has been introduced in Sec. IV C (dashed curves). Using the approximations that have been proposed, Eqs. (5) and (15) leads to a Mott-Gurney-type expression for the dilution-dependent current density of the

form

$$J(f_{\text{dil}}) \approx \alpha_1 \varepsilon_0 \varepsilon_r \frac{V^2}{L^3} \times \mu_{\text{ctr}} \left[c_{\text{act,ctr}} = \frac{c_{\text{tot,ctr}}(\alpha_2)}{(1 - f_{\text{dil}})}, f_{\text{dil}}, F_{\text{ctr}} \right], \quad (16)$$

where the μ_{ctr} function and $c_{\text{tot}}(\alpha_2)$ are given by Eq. (13) and Eq. (5), respectively, and where α_1 and α_2 are semiempirical parameters. This expression would be fully consistent with Eqs. (5) and (15) when taking $\alpha_1 = \alpha_2$. However, we find that by estimating the electron density in the device center using a value of α_2 that falls outside the range of values ($1 < \alpha < 2$) that would be expected for drift-only devices, a better description of the shape of the curves can be obtained. Most likely, this is due to an increase of the electron density in the devices due to charge-carrier diffusion. All dashed curves have been calculated with $\alpha_2 = 3.6$. We have taken $\alpha_1 = 1.5$, so that the current density for a device without traps and without dilutants coincides with the value from KMC simulations [$J = 1.2 \times 10^6$ A/m², see (a)]. The red curves show the results for the default parameter set that has been given in Table I.

Figure 6(a) shows the calculated and predicted dependence of the current density on the trap concentration. Excellent agreement is obtained for systems with strong dilution. For large trap concentrations, the mobility is strongly increased with dilution. With decreasing trap concentration, the fraction of dilutants above which all traps are filled is expected to decrease [Eq. (8)], leading to a decrease of the value of $f_{\text{dil,max}}$ at which the current density is largest. The simulation results indeed show such an effect. For a trap concentration of 0.1%, the peak has

almost vanished. For systems with 3% of traps the predicted current density is significantly larger than as would be expected. A similar but smaller deviation is found for the default system ($f_{\text{trap}} = 1\%$). We attribute that to field-enhanced direct trap-to-trap transport [see Fig. 2(b)]. That effect, which is not included in the model, will increase with increasing trap density. The effect will vanish for large f_{dil} , when a large fraction of the traps is filled.

Figures 6(b) and 6(c) show the effect of a variation of the voltage and the layer thickness, respectively. The simulation results are fairly well described by the approximate model. As expected from Eq. (8), the KMC simulations indeed show a decrease of the value of $f_{\text{dil,max}}$ with increasing voltage or when decreasing the layer thickness, caused by increased trap filling so that the trap-filled limit is already reached at a smaller dilution level.

In order to further demonstrate the generality of our methodology, the dilution-induced current enhancement is analyzed at a smaller dilution level. For a 50-nm-thick device, the KMC simulations, Fig. 6(c), show that the dilution-induced current-density enhancement has almost vanished. In the Supplemental Material [29], an analysis is given for these devices, using the methodology that has been used in Sec. IV. From Eq. (5), one expects that for a 50-nm device the total average electron density is a factor of four larger than for a 100-nm device. Figure S1 shows that due to this increase the nondiluted devices are already close to the trap-filled transport regime, and that for the most strongly diluted devices considered ($f_{\text{dil}} = 0.95$) trapping is expected to play only a minor role: in the device center, the density of electrons on transport sites is then more than a factor of 5 larger than

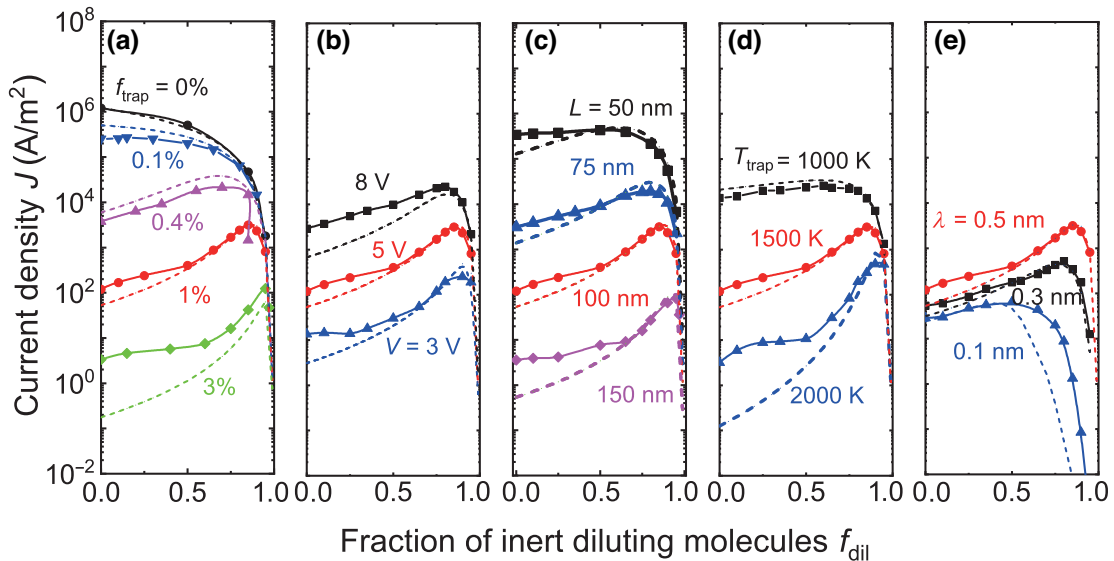


FIG. 6. Current density as a function of the fraction of inert diluting molecules for the device specified in Table I, obtained from 3D KMC FD simulations (symbols and full curves) and from an approximate model [Eq. (16), dashed curves], when varying (a) the fraction of traps (f_{trap}), (b) the applied voltage (V), (c) the device thickness (L), (d) the characteristic trap temperature (T_{trap}), and (e) the wave-function decay length (λ). The red curves show the result for the default parameter set.

the density of trapped electrons. Table SI gives a numerical analysis, similar to Table II for the 100-nm devices. The corresponding mobilities are shown in Fig. S2. Figure S2(a) shows that the slope of the mobility curves remains $(r - 1) \approx 4.17$. Figure S2(b) shows the mobility as a function of the total electron concentration, and explains why the initial dilution-induced current-density enhancement is very small. Due to the reduced role of trapped electrons trap-to-trap hopping does not play a strong role, so that the increase of the mobility with increasing field becomes much weaker than for the 100-nm devices [see Fig. S2(c)]. For the 50-nm devices, the decrease of the mobility with increasing dilution is therefore the dominant effect.

Figure 6(d) shows the effect of varying the width of the exponential trap DOS, which is proportional to the trap temperature T_{trap} . The distinction between transport and trap states decreases gradually with a decrease of T_{trap} . The reduction of the mobility due to traps is therefore strongly decreased when taking $T_{\text{trap}} = 1000$ K instead of 1500 K. The mobility reduction with increasing f_{dil} due to the enhanced average intermolecular distance becomes then the dominant effect, and the current-density increase almost vanishes. In contrast, for $T_{\text{trap}} = 2000$ K the reduction of the current density due to trapping is very strong, even though for small f_{dil} field-enhanced trap-to-trap transport leads to a larger current density than as would be expected from the model.

Figure 6(e) shows the sensitivity to a variation of the wave-function decay length λ . The model curves have been calculated using the λ -dependent mobility curves that are given in Fig. 4. When λ is decreased from 0.5 to 0.1 nm, nearest-neighbor hopping becomes the predominant process, instead of variable-range hopping. The resulting much stronger decrease of the free-electron mobility with f_{dil} (see Fig. 4) leads to a strong decrease of the current density for strong dilution, which sets already in at $f_{\text{dil}} \sim 0.5$. The decrease that is obtained from the KMC device simulations is less pronounced than as expected from the model, which uses the KMC mobility simulations. The difference may be due to incomplete relaxation of charge carriers to the trap states. A similar effect might more generally play a role in devices where the composition or measurement conditions lead to a small current density, e.g., in the case of large trap fraction or a large trap temperature.

Figure 6 suggests that the technique of active material dilution with an inert host can be used not only to improve the charge-transport efficiency, but also as a way of material parameter characterization. With well-controlled experiments, the shape of the $J(f_{\text{dil}})$ curves can provide information about the trap density, the width of the trap DOS, and, as demonstrated already for systems without traps by various authors [26,30,31], about the wave-function decay length. However, we remark that dilution by an inert material can cause changes of the transport material and trap densities of states, due to

conformational changes and due to the changed polarizability of the thin-film environment. This potential complication should be considered when predicting the effects of dilution from simulations and when analyzing experimental results.

V. MATERIALS WITH A GAUSSIAN DOS OF THE TRANSPORT OR TRAP MATERIAL

In this section we vary the DOS type by considering materials with Gaussian energetic disorder of the transport material and trap states with an exponential and Gaussian DOS [see Figs. 1(b) and 1(c)]. The simulations have been performed for the parameter values that are given in Table I, with $V = 5$ V.

Figure 7(a) shows the current density in systems without traps, obtained for three Gaussian disorder energies σ_T of the transport material. The introduction of disorder leads to a strong decrease of the mobility. However, the effect is for the relatively large value of λ used (0.5 nm) smaller than as expected from the variation of the mobility that has been obtained for $\lambda = 0.1$ nm [5,32]. The figure also shows that the dilution-induced decrease of the current density depends only weakly on σ_T .

The effect of adding the default exponential trap distribution ($f_{\text{trap}} = 0.01$ and $T_{\text{trap}} = 1500$ K) is shown in Fig. 7(b). For values of σ_T up to 0.05 eV, the dilution effect on the current density is almost independent of σ_T . This is due to two almost compensating effects. On the one hand, the electron mobility in the pure transport material decreases [see panel (a)]. On the other hand, an increasing disorder energy leads to a downward shift of the effective transport energy level (the mobility-determining highest energy level of molecular sites that still participate in the percolative transport process, see, e.g., Refs. [33,34]), so that the effective trap depth decreases. The figure shows that for nondiluted or weakly diluted devices with $\sigma_T = 0.10$ eV the latter effect even dominates: stronger disorder of the transport material leads then to a larger current density.

This somewhat counterintuitive result can be understood better by inspecting the variation of the electron concentration on transport sites (c_T) with the total electron concentration (c_{tot}), for various dilution fractions. Such functions shown in Eq. (17), calculated for simplicity under thermal equilibrium ($J = 0$) conditions, are shown for the various systems that are studied in this section in Fig. 8.

$$\begin{aligned} c_T &= (1 - f_{\text{dil}}) \int \frac{D_T(E)}{1 + \exp\left(\frac{E - E_F}{k_B T}\right)} dE, \\ c_{\text{tot}} &= (1 - f_{\text{dil}}) \int \frac{D_T(E) + D_{\text{trap}}(E)}{1 + \exp\left(\frac{E - E_F}{k_B T}\right)} dE, \end{aligned} \quad (17)$$

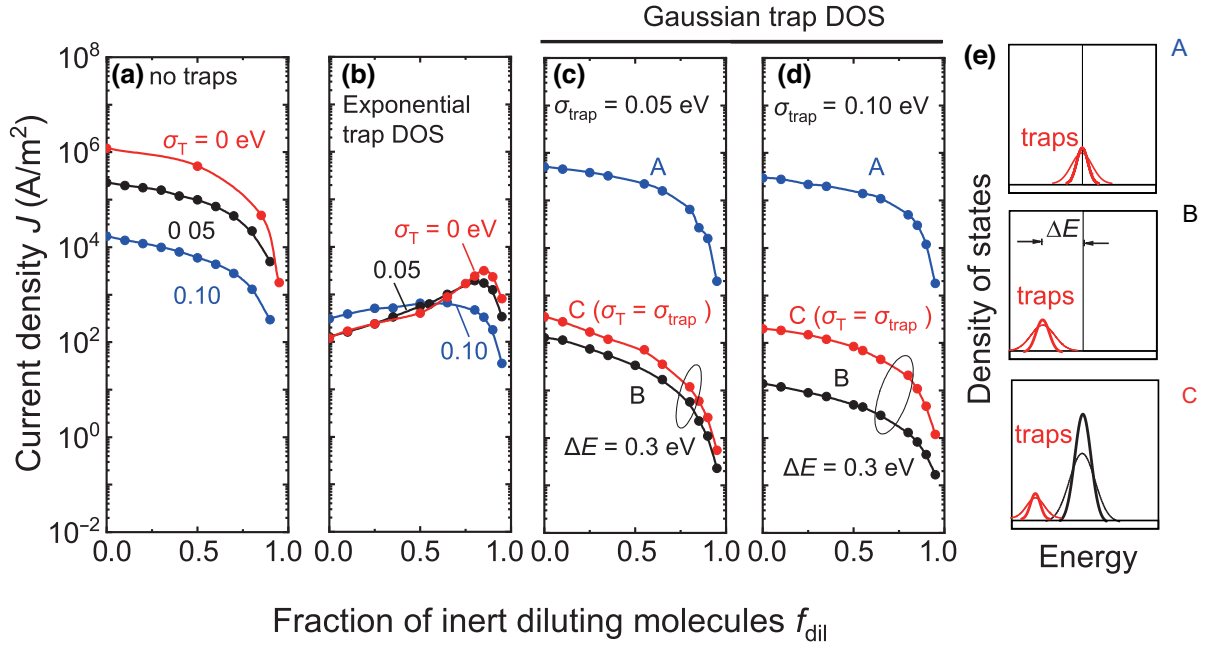


FIG. 7. Current density J at $V = 5$ V obtained from 3D KMC FD simulations as a function of the fraction of inert diluting molecules, f_{dil} , for transport materials with a Gaussian DOS with a width σ_T , as indicated. The simulation parameters that are not specific to the trap sites are as given in the first part (“Common parameters”) of Table I. (a) Transport material without traps. (b) Systems with an exponential trap DOS ($f_{\text{trap}} = 0.01$ and $T_{\text{trap}} = 1500$ K). (c),(d) Systems with a Gaussian trap DOS with $f_{\text{trap}} = 0.01$ and σ_{trap} as indicated, for the DOS types that are shown in panel (e). For DOS-types B and C, the trap depth is $\Delta E = 0.3$ eV.

with $D_T(E)$ and $D_{\text{trap}}(E)$ the DOS for transport and trap materials, respectively, which could be δ , exponential, or Gaussian shaped. E_F is obtained implicitly given c_{tot} . Panel (a) shows these functions for two of the systems that are studied in Fig. 7(b), with $\sigma_T = 0$ and 0.10 eV. The dilution fraction $f_{\text{dil}} = 0$ is varied in steps of 0.2, from 0 to 0.8, as indicated by the arrows. The gray zone indicates the approximate value of c_{tot} in the device center, which is determined by the voltage and the device thickness [see Eq. (5)]. The figure shows that c_T is indeed for systems with $\sigma_T = 0.10$ eV (red curves) significantly larger than for systems with $\sigma_T = 0$ eV (black curves). The figure also shows that for $\sigma_T = 0.10$ eV systems significant trap filling leads to a much smaller sensitivity of c_T to dilution than for $\sigma_T = 0$ eV. Also for $\sigma_T = 0.05$ eV systems (not shown in the figure) no significant trap filling is expected for dilution fractions up to 0.8. This explains the finding that for the $\sigma_T = 0.10$ eV devices the sensitivity of the current density due to dilution is much smaller than for the $\sigma_T = 0$ or 0.05 eV devices.

Figures 7(c) and 7(d) show the sensitivity to dilution for systems with a Gaussian trap DOS with a width σ_T , for the three DOS types that are shown in panel (e). For DOS-types B and C an average trap depth $\Delta E = 0.3$ eV is taken. For none of these cases a dilution-induced increase of the current density is observed. This finding can be understood from the $c_T(c_{\text{tot}}, f_{\text{dil}})$ curves that are shown in Figs. 8(b) and 8(c), for widths of the trap DOS of 0.05 and 0.10 eV,

respectively. These figures show that for the Gaussian trap DOS cases studied the sensitivity of $c_T(c_{\text{tot}}, f_{\text{dil}})$ to a change of the dilution fraction is very small as compared to that for the exponential DOS cases studied. One should in all cases focus on the results for c_{tot} values in the gray-shaded zones.

The shapes of the $c_T(c_{\text{tot}}, f_{\text{dil}})$ curves are for systems with a Gaussian trap DOS and for small total electron concentrations fundamentally different from those for an exponential trap DOS, shown in panel (a). The difference may be understood by considering the difference in the increase of the average electron energy when filling an exponential or Gaussian trap DOS. In the case of an exponential trap DOS, the average electron energy increases continuously, leading to a continuous decrease of the energy distance to the transport level and hence to an increase of the ratio c_T/c_{tot} . However, in the case of a Gaussian trap DOS the average electron energy is for small electron concentrations constant and equal to $E_{\text{LUMO,trap}} - E_{\text{th,eq}}$, where $E_{\text{LUMO,trap}}$ is the average LUMO energy of the trap states and $E_{\text{th,eq}} = \sigma_{\text{trap}}^2/(k_B T)$ is the thermal equilibrium energy. In this “independent particle” (Boltzmann) regime, the ratio c_T/c_{tot} remains constant. A crossover to a regime within which the average energy increases with increasing filling of the DOS takes place around a concentration $c_{\text{tot},1} \approx (N_{\text{trap}}/2) \exp\{-[\sigma_{\text{trap}}/(k_B T)]^2/2\}$ [35]. The trap-filled regime is reached at $c_{\text{tot},2} \approx N_{\text{trap}}$. This range is indicated in panel (c) by the two vertical dashed lines. Dashed lines are also used to indicate the variation of

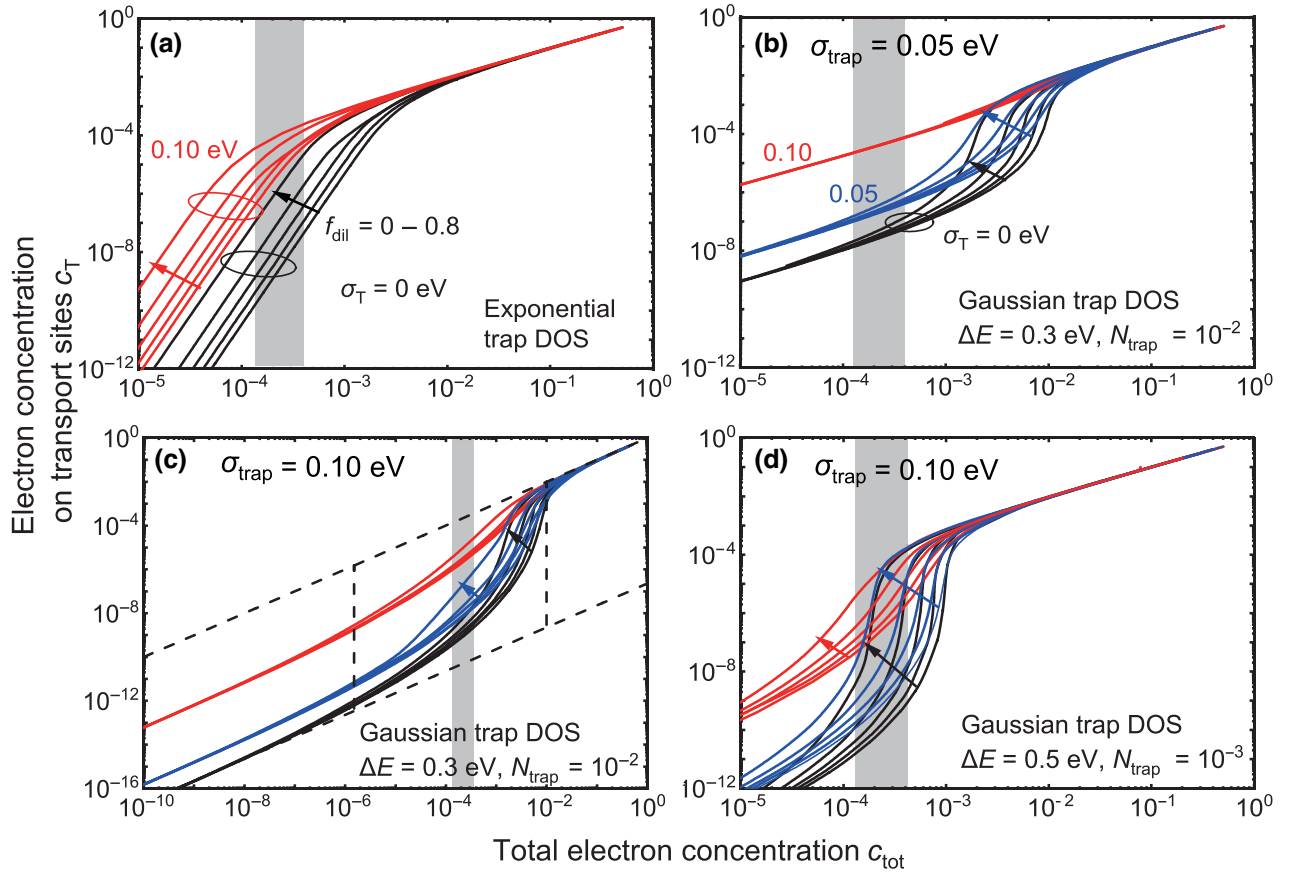


FIG. 8. Dependence of the thermal equilibrium electron concentration on transport sites, c_T , on the total electron concentration, c_{tot} , calculated from Eq. (17), for (a) systems with an exponential trap DOS, studied in Fig. 7(b), and (b)–(d) systems with a Gaussian trap DOS, with parameters that are specified in the figures. Panels (b),(c) refer to panels (c),(d), respectively, of Fig. 7. Curves are given for transport materials with $\sigma_T = 0$ eV (black), 0.05 eV (blue), and 0.10 eV (red), and for dilution fractions f_{dil} increasing from 0 to 0.8 in steps of 0.2, in the direction of the arrows. The gray zones indicate the region of total charge concentrations around the value of $(1.4 - 4) \times 10^{-4}$ that is approximately found in the device center of 100-nm devices, studied at 5 V (see Tables II and SI [29]). The vertical dashed lines in panel (c) mark the boundaries $c_{\text{tot},1}$ and $c_{\text{tot},2}$ of the intermediate concentration range in which the largest sensitivity of the current density to f_{dil} is expected (see the text in Sec. V). Dashed curves with a slope of 1 on the double-log scale used show the (partially extrapolated) $c_T(c_{\text{tot}})$ functions in the Boltzmann and trap-filled regimes for $\sigma_T = 0$ eV materials. Panel (d) shows a set of curves for parameters for which a strong trap dilution effect is expected.

$c_T(c_{\text{tot}})$ in the independent-particle and trap-filled regimes, with on the double-log scale used a slope of 1.

Figures 8(b) and 8(c) suggest that also for devices that are based on transport and trap materials with a Gaussian DOS an increase of the current density with dilution could be observed. Such an effect can be attained by fine tuning N_{trap} , which determines the concentration $c_{\text{tot},2}$ at which the trap-filled regime is reached, and by fine tuning c_{tot} , which depends on the voltage and layer thickness [see Eq. (5)]. It will also be helpful to minimize σ_T and to use a large trap depth. As an example, Fig. 8(d) shows that a strong dilution effect is expected for systems with $N_{\text{trap}} = 10^{-3}$, so that the $c_T(c_{\text{tot}})$ curves increase steeply in the range $c_{\text{tot}} = 10^{-4} - 10^{-3}$, and with a trap depth of 0.5 eV. Well-controlled evaporation deposition of films with such a small guest concentration is in practice not

easy. However, solution processing is expected to provide a feasible alternative.

VI. SUMMARY, CONCLUSIONS, AND OUTLOOK

We have performed a systematic 3D KMC simulation study on the dilution-induced change of the current density in symmetric unipolar single-layer devices that are based on disordered organic semiconductors. For systems containing traps with an exponential DOS, a distinct dilution-induced increase of the current density can occur, consistent with experimental observations. The effect is determined by a balance between the positive effect of trap dilution, which continues with increasing f_{dil} until the trap-filled limit has been reached, and the negative effect of a decrease of the mobility of the transport material

with increasing dilution. An approximate semiquantitative model has been shown to provide a fair description of the sensitivity of the effect to various changes of the material parameters, the voltage, and the layer thickness.

For systems with a Gaussian shape of the trap DOS, the effect is only expected to occur for fine-tuned combinations of the material parameters and measurement conditions, leading to a total charge density in the bulk of the device that is close to the value at which the trap-filled limit is reached.

Potentially, the trap-dilution technique can be used to characterize various material parameters, such as the wave-function decay length. It would for such quantitative applications be of interest to refine the KMC methods that have been used in this work, by extending them to diluted networks with both positional and energetic disorder [32,34]. It would also be important to gain improved understanding of the effect of dilution on the material parameters, such as the energy levels and the disorder energies σ , using molecular dynamics and quantum chemical calculations [1,3].

The trap-dilution technique provides new degrees of freedom for fine tuning the device performance of small-molecule multilayer OLEDs, by applying it to a specific layer or by using the concentration grading technique [36,37]. One application would be related to the electron-transport layers (ETLs). Electron-transport materials show often a relatively low electron mobility due to the presence of an extrinsic exponential trap DOS. The resulting electron-hole mobility imbalance can lead to strongly nonuniform exciton generation in the emissive layer, in a thin zone near the interface with the electron-transport layer (ETL), leading to a large efficiency rolloff and a shortened operational lifetime. In such a case, application of the trap dilution technique to the ETL could improve the device characteristics, and 3D KMC simulations could be used to explore the huge design space.

ACKNOWLEDGMENTS

This work was supported by the National Key R&D Program of China (Grant No. 2023YFB36113001), the talents project of Guangdong Province, National Natural Science Foundation of China (Grant No. 62005083), Science and Technology Program of Guangzhou (Grant No. 2019050001), the leading talents of Guangdong Province Program (Grant No. 00201504), Program for Chang Jiang Scholars and Innovative Research Teams in Universities (Grant No. IRT 17R40), Guangdong Provincial Key Laboratory of Optical Information Materials and Technology (Grant No. 2023B1212060065), National Center for International Research on Green Optoelectronics, MOE International Laboratory for Optical Information Technologies and the 111 Project.

- [1] P. Friederich, F. Symalla, V. Meded, T. Neumann, and W. Wenzel, Ab initio treatment of disorder effects in amorphous organic materials: toward parameter free materials simulation, *J. Chem. Theory Comput.* **10**, 3720 (2014).
- [2] P. Friederich, V. Meded, A. Poschlad, T. Neumann, V. Rodin, V. Stehr, F. Symalla, D. Danilov, G. Lüdemann, R. F. Fink, I. Kondov, F. von Wrochem, and W. Wenzel, Molecular origin of the charge carrier mobility in small molecule organic semiconductors, *Adv. Funct. Mater.* **26**, 5757 (2016).
- [3] P. Kordt, J. J. M. van der Holst, M. Al Helwi, W. Kowalsky, F. May, A. Badinski, C. Lennartz, and D. Andrienko, Modeling of organic light emitting diodes: from molecular to device properties, *Adv. Funct. Mater.* **25**, 1955 (2015).
- [4] F. May, B. Baumeier, C. Lennartz, and D. Andrienko, Can lattice models predict the density of states of amorphous organic semiconductors? *Phys. Rev. Lett.* **109**, 136401 (2012).
- [5] R. Coehoorn and P. A. Bobbert, Effects of Gaussian disorder on charge carrier transport and recombination in organic semiconductors, *Phys. Stat. Sol. (a)* **209**, 2354 (2012).
- [6] P. W. Blom and M. Vissenberg, Charge transport in poly(p-phenylene vinylene) light-emitting diodes, *Mater. Sci. Eng. R Rep.* **27**, 53 (2000).
- [7] M. M. Mandoc, B. de Boer, G. Paasch, and P. W. M. Blom, Trap-limited electron transport in disordered semiconducting polymers, *Phys. Rev. B* **75**, 193202 (2007).
- [8] N. B. Kotadiya, A. Mondal, P. W. Blom, D. Andrienko, and G.-J. A. Wetzelaer, A window to trap-free charge transport in organic semiconducting thin films, *Nat. Mater.* **18**, 1182 (2019).
- [9] M. C. J. M. Vissenberg and M. Matters, Theory of the field-effect mobility in amorphous organic transistors, *Phys. Rev. B* **57**, 12964 (1998).
- [10] N. Tessler and Y. Roichman, Amorphous organic molecule/polymer diodes and transistors – comparison between predictions based on Gaussian or exponential density of states, *Org. Electron.* **6**, 200 (2005).
- [11] B. Ramachandran, H. G. A. Huizing, and R. Coehoorn, Charge transport in metal/semiconductor/metal devices based on organic semiconductors with an exponential density of states, *Phys. Rev. B* **73**, 233306 (2006).
- [12] J. O. Oelerich, D. Hümmer, and S. D. Baranovskii, How to find out the density of states in disordered organic semiconductors, *Phys. Rev. Lett.* **108**, 226403 (2012).
- [13] P. Mark and W. Helfrich, Space-charge-limited currents in organic crystals, *J. Appl. Phys.* **33**, 205 (1962).
- [14] D. Abbaszadeh, A. Kunz, G. Wetzelaer, J. J. Michels, N. Crăciun, K. Koynov, I. Lieberwirth, and P. W. Blom, Elimination of charge carrier trapping in diluted semiconductors, *Nat. Mater.* **15**, 628 (2016).
- [15] D. Abbaszadeh and P. W. M. Blom, Efficient blue polymer light-emitting diodes with electron-dominated transport due to trap dilution, *Adv. Electron. Mater.* **2**, 1500406 (2016).
- [16] The 3D-KMC tool used in this work is Bumblebee, provided by Simbeyond B.V. (simbeyond.com).
- [17] M. Mesta, M. Carvelli, R. J. De Vries, H. van Eersel, J. J. van der Holst, M. Schober, M. Furno, B. Lüssem, K. Leo, P. Loeb, *et al.*, Molecular-scale simulation of electroluminescence in a multilayer white organic light-emitting diode, *Nat. Mater.* **12**, 652 (2013).

- [18] H. van Eersel, P. Bobbert, R. Janssen, and R. Coehoorn, Monte Carlo study of efficiency roll-off of phosphorescent organic light-emitting diodes: Evidence for dominant role of triplet-polaron quenching, *Appl. Phys. Lett.* **105**, 143303 (2014).
- [19] R. Coehoorn, H. Van Eersel, P. Bobbert, and R. Janssen, Kinetic Monte Carlo study of the sensitivity of OLED efficiency and lifetime to materials parameters, *Adv. Funct. Mater.* **25**, 2024 (2015).
- [20] S. Gottardi, M. Barbry, R. Coehoorn, and H. van Eersel, Efficiency loss processes in hyperfluorescent OLEDs: A kinetic Monte Carlo study, *Appl. Phys. Lett.* **114**, 073301 (2019).
- [21] A. Miller and E. Abrahams, Impurity conduction at low concentrations, *Phys. Rev.* **120**, 745 (1960).
- [22] F. Liu, Y. Su, X. Lin, L. Nian, B. Wu, Q. Niu, H. Van Eersel, P. A. Bobbert, R. Coehoorn, and G. Zhou, Image-force-stabilized interfacial dipole layer impedes charge injection into disordered organic semiconductors, *Phys. Rev. Appl.* **17**, 024003 (2022).
- [23] S. Van Mensfoort, R. De Vries, V. Shabro, H. Loebel, R. Janssen, and R. Coehoorn, Electron transport in the organic small-molecule material BAQ – the role of correlated disorder and traps, *Org. Electron.* **11**, 1408 (2010).
- [24] A. M. Stoneham, Current injection in solids, *Phys. Bull.* **21**, 558 (1970).
- [25] M. Vissenberg and M. Matters, Theory of the field-effect mobility in amorphous organic transistors, *Phys. Rev. B* **57**, 12964 (1998).
- [26] O. Rubel, S. Baranovskii, P. Thomas, and S. Yamasaki, Concentration dependence of the hopping mobility in disordered organic solids, *Phys. Rev. B* **69**, 014206 (2004).
- [27] J. Zhou, Y. Zhou, J. Zhao, C. Wu, X. Ding, and X. Hou, Carrier density dependence of mobility in organic solids: A Monte Carlo simulation, *Phys. Rev. B* **75**, 153201 (2007).
- [28] F. Liu, H. van Eersel, B. Xu, J. G. Wilbers, M. P. de Jong, W. G. van der Wiel, P. A. Bobbert, and R. Coehoorn, Effect of Coulomb correlation on charge transport in disordered organic semiconductors, *Phys. Rev. B* **96**, 205203 (2017).
- [29] See the Supplemental Material at <http://link.aps.org/supplemental/10.1103/PhysRevApplied.21.014050> for additional simulation results of the charge-carrier profile, charge-carrier concentration, and electric-field-dependent mobility, and the analysis of dilution induced current enhancement for a 50-nm-thick device.
- [30] B. Ries, H. Bässler, and M. Silver, Pseudo-percolation of charge carriers in molecularly doped polymers: A Monte Carlo study, *Philos. Mag. B* **54**, 141 (1986).
- [31] J. M. Sin and Z. G. Soos, Hopping transport in molecularly doped polymers: Joint modelling of positional and energetic disorder, *Philos. Mag.* **83**, 901 (2003).
- [32] H. Bässler, Charge transport in disordered organic photoconductors – a Monte Carlo simulation study, *Phys. Stat. Sol. (b)* **175**, 15 (1993).
- [33] D. Monroe, Hopping in exponential band tails, *Phys. Rev. Lett.* **54**, 146 (1985).
- [34] J. Cottaar, L. Koster, R. Coehoorn, and P. Bobbert, Scaling theory for percolative charge transport in disordered molecular semiconductors, *Phys. Rev. Lett.* **107**, 136601 (2011).
- [35] R. Coehoorn, W. F. Pasveer, P. A. Bobbert, and M. A. J. Michels, Charge-carrier concentration dependence of the hopping mobility in organic materials with Gaussian disorder, *Phys. Rev. B* **72**, 155206 (2005).
- [36] F. Lindla, M. Boesing, C. Zimmermann, F. Jessen, P. Van Gemmen, D. Bertram, D. Keiper, N. Meyer, M. Heuken, H. Kalisch, *et al.*, Highly efficient yellow organic light emitting diode based on a layer-cross faded emission layer allowing easy color tuning, *Appl. Phys. Lett.* **95**, 213305 (2009).
- [37] J. Lee, H.-F. Chen, T. Batagoda, C. Coburn, P. I. Djurovich, M. E. Thompson, and S. R. Forrest, Deep blue phosphorescent organic light-emitting diodes with very high brightness and efficiency, *Nat. Mater.* **15**, 92 (2016).